

UCSF

UC San Francisco Previously Published Works

Title

An appliance for monitoring the shrinkage of root caries with OCT.

Permalink

<https://escholarship.org/uc/item/7js0m6r7>

Authors

Yang, Vincent B
Fried, Daniel

Publication Date

2019-02-01

DOI

10.1117/12.2512933

Peer reviewed

PROCEEDINGS OF SPIE

SPIDigitalLibrary.org/conference-proceedings-of-spie

An appliance for monitoring the shrinkage of root caries with OCT

Vincent B. Yang, Daniel Fried

Vincent B. Yang, Daniel Fried, "An appliance for monitoring the shrinkage of root caries with OCT," Proc. SPIE 10857, Lasers in Dentistry XXV, 108570L (28 February 2019); doi: 10.1117/12.2512933

SPIE.

Event: SPIE BiOS, 2019, San Francisco, California, United States

An appliance for monitoring the shrinkage of root caries with OCT

Vincent B. Yang and Daniel Fried
University of California, San Francisco, San Francisco, CA 94143-0758

ABSTRACT

Demineralized root dentin and cementum are mostly collagen that shrinks significantly upon dehydration. Active root caries lesions manifest shrinkage upon dehydration, however during the remineralization of root caries lesions mineral is deposited on the outside of the lesion arresting the lesion and arrested lesions no longer manifest shrinkage upon dehydration. Optical coherence tomography is ideally suited for the measurement of that shrinkage for the assessment of lesion activity. In this study the shrinkage of natural root caries lesions on extracted teeth were measured using a CP-OCT system with a 3D printed appliance with an integrated air nozzle suitable for clinical use.

Keywords: optical coherence tomography, root caries, shrinkage, lesion activity

1. INTRODUCTION

Clinical diagnosis of root caries is highly subjective and is based on visual and tactile parameters. In contrast to coronal caries, root caries lacks a valid diagnostic standard, such as radiography [1]. Moreover, early root caries lesions are much more difficult to detect than the early incipient white spot lesions seen with coronal caries. There are often no clinical symptoms with root caries, although pain may be present in advanced lesions. Traditional methods of visual-tactile diagnosis for root caries can result in a correct diagnosis, but not until the lesion is at an advanced stage [1]. In addition, investigators have not developed a reliable relationship between lesion appearance and activity [2-4]. Even though most experts agree that active root lesions are soft, tactile hardness assessments remain subjective and lack reliability [2]. Multifactorial root caries scoring systems have been developed with mixed success [5, 6]. More recently, the International Caries Detection and Assessment System (ICDAS) coordinating committee and Ekstrand et al. proposed clinical scoring systems for assessing root caries lesion activity [5, 7]. Criteria include: color (light /dark brown, black); Texture (smooth, rough); Appearance (shiny or glossy, matte or non-glossy); Tactile (soft, leathery, hard); Cavitation (loss of anatomical contour); and proximity to the gingival margin [8]. However, such clinical methods for root caries lesion activity assessment lack histological validation and are composed of only visual and tactile exams, which are prone to subjective bias and interference from staining [9]. Histological analyses for lesion assessment such as transverse microradiography (TMR) and polarized light microscopy (PLM) require destruction of the tooth and are not suitable for use *in vivo*. Incorrect diagnosis can result in under treatment or over treatment. If a decision to restore is made prematurely when remineralization was feasible, the patient is committed to a restoration, or replacement restorations, that can become progressively larger. If the lesion is active and intervention is delayed, often the patient will require a root canal or extraction.

CP-OCT is uniquely capable of showing structural changes such as the formation of a zone of increased mineral density and reduced light scattering due to remineralization that indicates that the lesion is arrested [10-12] and that a distinct transparent surface zone has been formed [11, 13].

Although the penetration depth of near-IR light is limited in dentin compared to enamel, high quality images of early root caries and demineralization in dentin are feasible [14]. CP-OCT has been used successfully to measure demineralization in simulated caries models in dentin and on root surfaces (cementum) [12, 15, 16]. CP-OCT has also been used to measure remineralization on dentin surfaces and to detect the formation of a highly mineralized layer on the lesion surface after exposure to a remineralization solution [16]. Cementum has lower reflectivity than dentin in OCT images, making it possible to easily discriminate the remaining cementum thickness [15, 16]. OCT has also been used to help discriminate between noncarious cervical lesions and root caries *in vivo* [17]. Kaneko et al. and Zakian et al. [18, 19] demonstrated that lesions on coronal surfaces could be differentiated from sound

enamel in thermal images. We recently demonstrated that thermal imaging via dehydration can be used to assess lesion activity on both enamel [20] and dentin [21] surfaces.

OCT is ideally suited for measuring dimensional changes in the tooth. Shrinkage occurs in demineralized dentin due to the loss of water from the collagen matrix with dehydration. More severe lesions manifest greater shrinkage while lesions that have been successfully remineralized and have formed an intact highly mineralized surface zone have reduced shrinkage [16]. There was a correlation between the lesion severity and the degree of shrinkage measured using OCT [12]. Upon remineralization, such lesions expanded to the original contours and no longer manifested shrinkage [12].

This suggests that the degree of shrinkage of root caries lesions can serve as an indicator of severity and help discriminate between active and arrested root caries lesions. Recently the shrinkage of natural caries lesions on extracted teeth was measured with OCT [22]. In this study we used a 3D printer to print an appliance that was attached to a CP-OCT handpiece for the *in vivo* monitoring of shrinkage and tested the device *ex vivo* on both simulated and natural lesions on root surfaces.



Fig. 1. 3D printed prototype appliance for use with the CP-OCT handpiece. The window is centered over the lesion and forced air is delivered through the cylindrical shaped channel to the window.

2. MATERIALS AND METHODS

2.1 Sample preparation

Teeth extracted from patients in the San Francisco Bay Area were collected, cleaned, sterilized with gamma radiation, and stored in a 0.1% thymol solution. These teeth were then sliced into 2-3 mm dentin slices in the axial direction, and these slices were halved in the apical direction. These slices were examined to make sure that there were no natural lesions or calculus on them. These slices were mounted on 1.2 x 3 cm rectangular blocks of black orthodontic composite resin with the outward tooth dentin surface facing up. The surface of the dentin was then divided into two windows, using acid-resistant varnish (red nail polish;

Revlon, New York, NY), in order to demarcate the boundary of the eventual generated lesions. Each rectangular block fit precisely in an optomechanical assembly that could be positioned with micron accuracy.

Artificial dentin lesions were prepared using a demineralization solution maintained at 37°C at pH 4.9. The solution consists of 40 mL aliquots of 2.0 mmol/L phosphate, 2.0 mmol/L calcium, and 0.075 mol/L acetate. Ten samples each with two windows were placed in this solution for 7 days. After the time was up, samples were taken from the solution, rinsed with deionized water, and stored in a 0.1% thymol solution for further examination. Five teeth with natural root lesions were also used.

2.2 Cross-Polarization Optical Coherence Tomography (CP-OCT)

The cross-polarization OCT system used for this study was purchased from Santec (Komaki, Aichi, Japan). This system acquires only the cross polarization image (CP-OCT), not both the cross and co-polarization images (PS-OCT). The Model IVS-3000-CP utilizes a swept laser source; Santec Model HSL-200-30 operating with a 30 kHz a-scan sweep rate. The Mac-Zehnder interferometer is integrated into the handpiece which also contains the microelectromechanical (MEMS) scanning mirror and the imaging optics. It is capable of acquiring complete tomographic images of a volume of 6 x 6 x 7 mm in approximately 3 seconds. The body of the handpiece is 7 x 18 cm with an imaging tip that is 4 cm long and 1.5 cm across. This system operates at a wavelength of 1321-nm with a bandwidth of 111-nm with a measured resolution in air of 11.4 μm (3 dB). The lateral resolution is 80- μm ($1/e^2$) with a transverse imaging window of 6 mm x 6 mm and a measured imaging depth of 7-mm in air. The polarization extinction ratio was measured to be 32 dB.

We printed appliances that fit over the end of the CP-OCT scanner using a Formlabs 2 printer (Somerville, MA) and black, white and Dental SG resins. The Dental SG resin is autoclavable. An example of a printed appliance is shown in Fig. 1. For infection control the entire CP-OCT handpiece is covered in polypropylene film and the appliance is placed over that film and the appliance is placed directly in contact with the tooth surface. A nozzle is attached to the appliance to provide air to both dehydrate the lesion area and prevent fogging of the scanning window.

2.3 Shrinkage Measurements

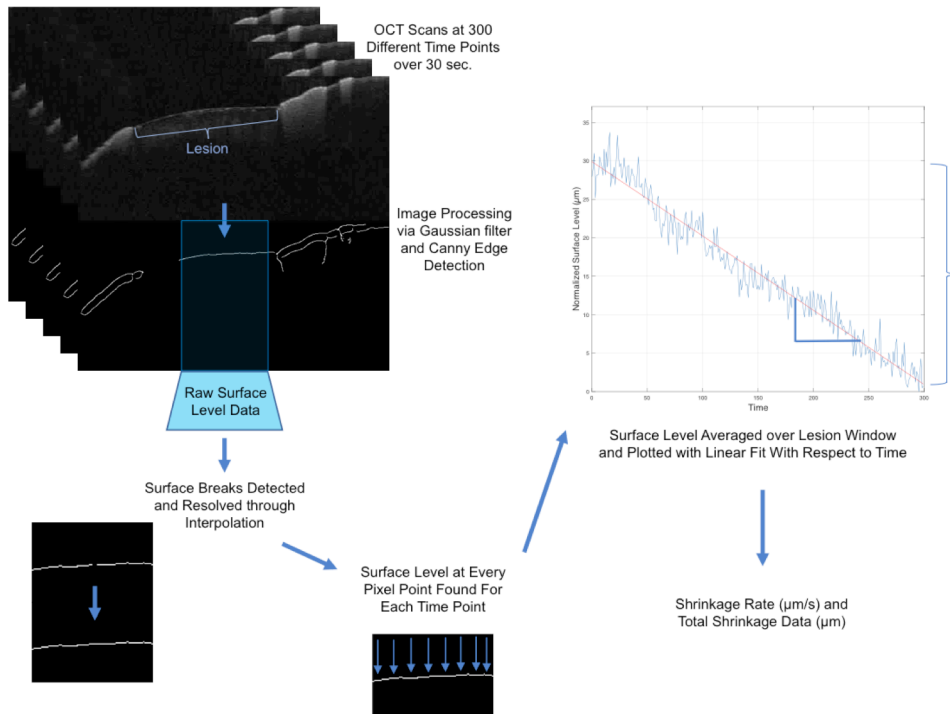


Fig. 2. Outline of steps taken in the processing of OCT images for the measurement of lesion shrinkage.

Shrinkage measurements were taken on extracted teeth with the probe and polypropylene film in place to emulate clinical imaging. The inlet pressure for the airflow through the nozzle was maintained at either 15, 20 or 25 psi for the duration of the drying process. Drying was done for 30 seconds and the sample was continuously scanned as a two-dimensional slice (Fig. 2) in real time.

The captured videos were then extracted and processed into frames. For the duration of 30 seconds, each video was recorded at 10 frames per second resulting in 300 total frames. These frames were then batch-imported into Matlab from Mathworks, Inc. (Natick, MA), in the form of images. Each image-frame was cropped to the lesion window and filtered using a Gaussian filter (5x5) to mitigate noise. Surface detection was done using a Canny edge detection algorithm (threshold = [0.1 0.25]), revealing the surface line, and the level of this surface was arrayed for each frame. The steps taken to acquire and process the shrinkage data are outlined in Fig. 2. Any surface breaks, null or outlier, were resolved via interpolation to maintain consistency. Once the surface level over the chosen lesion window was recorded at each time point, this level was averaged for each time point. The minimum average surface level was represented as 0, and the remaining surface levels were scaled with this in mind, resulting in a value representing the level of the surface at each time point.

Using frames of sample shrinkage from consistent drying over the span of thirty seconds, measurements were carried out through the detection of the average point level of the surface spanning the artificial lesion window.

2.4 Lesion Thickness Measurements

OCT images were acquired at three different time points: at the start of drying, after thirty seconds elapsed, and after two minutes elapsed. For each snapshot, vertical line profiles were taken for each pixel width over the whole lesion window to find the apparent thickness of the lesion. Thickness was found through the $1/e^2$ intersection relative to the maximum intensity in the signal of the lesion, denoting the apparent edges where the signal can be considered to be

part of the lesion. Measurements were averaged to find the mean thickness of the lesion. The thickness of each lesion was averaged for each air pressure (15, 20, and 25 psi), and each sample type (simulated and artificial).

3. RESULTS AND DISCUSSION

Figure 3 shows CP-OCT b-scans images acquired from simulated and natural root caries lesions before and after shrinkage indicating that the changes can be clearly measured using the appliance.

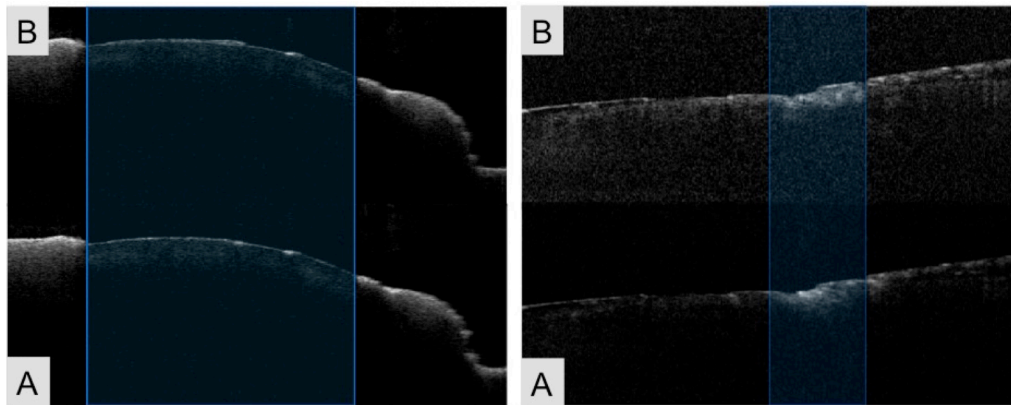


Fig. 3. CP-OCT scans of before (B) and after (A) drying simulated (left) and natural (right) lesions on root surfaces. Shrinkage was measured in the shaded blue area.

Lesion activity is an important characteristic to consider, because it determines whether treatment should be given or withheld. Histological analyses for lesion assessment such as transverse microradiography (TMR) and polarized light microscopy (PLM) require destruction of the tooth and are not suitable for use *in-vivo*, while OCT has been demonstrated for clinical *in-vivo* use. Incorrect diagnosis can result in undertreatment or overtreatment. If a decision to restore is made prematurely when remineralization was feasible, the patient is committed to a restoration and often replacement restorations that become progressively larger. If the lesion is active and intervention is delayed, often the patient will require a more invasive and expensive restorative procedure. Shrinkage can potentially be used as a marker for lesion activity and to indicate that remineralization has taken place. Mineral deposition in the pores near the surface of the lesion during remineralization increases the mineral content near the surface and forms a surface layer. This highly mineralized surface layer reduces the permeability of fluids preventing further demineralization and remineralization arresting lesion progression and repair. We plan to use the appliance in future clinical studies to measure the shrinkage of root caries lesions *in vivo*.

4. ACKNOWLEDGEMENTS

The authors acknowledge the support of the California Tobacco-Related Disease Research Program (TRDRP) and NIH/NIDCR Grant R01-DE027335.

5. REFERENCES

- [1] D. W. Banting, Diagnosis of Root Caries NIH Consensus Statement, (2001).
- [2] D. W. Banting, "Diagnosis and prediction of root caries," *Adv Dent Res*, 7(2), 80-6 (1993).
- [3] P. Hellyer, D. Beighton, M. Heath, and E. Lynch, "Root caries in older people attending a general practice in East Sussex," *Brit Dent J* 169, 201-206 (1990).
- [4] M. Schaeken, H. Keltjens, and J. Van der Hoeven, "Effects of fluoride and chlorhexidine on the microflora of dental root surfaces and progression of root-surface caries," *J Dent Res*, 70, 150-153 (1991).

- [5] K. Ekstrand, S. Martignon, and P. Holm-Pedersen, "Development and evaluation of two root caries controlling programmes for home-based frail people older than 75 years," *Gerodontology*, 25(2), 67-75 (2008).
- [6] O. Fejerskov, W. M. Luan, B. Nyvad, E. Budtz-Jorgensen, and P. Holm-Pedersen, "Active and inactive root surface caries lesions in a selected group of 60- to 80-year-old Danes," *Caries Res*, 25(5), 385-91 (1991).
- [7] A. Ismail, D. Banting, H. Eggertsson, K. Ekstrand, A. Ferreira-Zandona, C. Longbottom, N. Pitts, E. Reich, D. Ricketts, R. Selwitz, W. Sohn, G. Topping, and D. Zero, "Rationale and evidence for the International Caries Detection and Assessment System (ICDAS II)," In *Proceedings of the 7th Indiana Conference*. Indiana University, Vol. 4, 161-221 (2005).
- [8] N. Pitts, *Detection, Assessment, Diagnosis and Monitoring of Caries*, Monographs in Oral Science Vol. 21 Karger, Basel (2009).
- [9] E. Lynch, and D. Beighton, "A comparison of primary root caries lesions classified according to colour," *Caries Res*, 28(4), 233-9 (1994).
- [10] R. S. Jones, C. L. Darling, J. D. Featherstone, and D. Fried, "Remineralization of in vitro dental caries assessed with polarization-sensitive optical coherence tomography," *J Biomed Optics*, 11(1), 014016 (2006).
- [11] R. S. Jones, and D. Fried, "Remineralization of enamel caries can decrease optical reflectivity," *J Dent Res*, 85(9), 804-8 (2006).
- [12] S. K. Manesh, C. L. Darling, and D. Fried, "Nondestructive assessment of dentin demineralization using polarization-sensitive optical coherence tomography after exposure to fluoride and laser irradiation," *J Biomed Mater Res B Appl Biomater*, 90(2), 802-12 (2009).
- [13] H. Kang, C. L. Darling, and D. Fried, "Nondestructive monitoring of the repair of enamel artificial lesions by an acidic remineralization model using polarization-sensitive optical coherence tomography," *Dent Mat*, 28(5), 488-494 (2012).
- [14] B. T. Amaechi, A. G. Podoleanu, G. Komarov, S. M. Higham, and D. A. Jackson, "Quantification of root caries using optical coherence tomography and microradiography: a correlational study," *Oral Health Prev Dent*, 2(4), 377-82 (2004).
- [15] C. Lee, C. Darling, and D. Fried, "Polarization Sensitive Optical Coherence Tomographic Imaging of Artificial Demineralization on Exposed Surfaces of Tooth Roots," *Dent Mat*, 25(6), 721-728 (2009).
- [16] S. K. Manesh, C. L. Darling, and D. Fried, "Polarization-sensitive optical coherence tomography for the nondestructive assessment of the remineralization of dentin," *J Biomed Optics*, 14(4), 044002 (2009).
- [17] I. Wada, Y. Shimada, M. Ikeda, A. Sadr, S. Nakashima, J. Tagami, and Y. Sumi, "Clinical assessment of non carious cervical lesion using swept-source optical coherence tomography," *J Biophotonics*, 8(10), 846-54 (2015).
- [18] K. Kaneko, K. Matsuyama, and S. Nakashima, "Quantification of Early Carious Enamel Lesions by using an Infrared Camera," *Early detection of Dental caries II*. Indiana University, Vol. 1 483-99 (1999).
- [19] C. M. Zakian, A. M. Taylor, R. P. Ellwood, and I. A. Pretty, "Occlusal caries detection by using thermal imaging," *J Dentistry*, 38(10), 788-795 (2010).
- [20] R. C. Lee, C. L. Darling, and D. Fried, "Assessment of remineralization via measurement of dehydration rates with thermal and near-IR reflectance imaging," *J Dent*, 43, 1032-1042 (2015).
- [21] R. C. Lee, C. L. Darling, and D. Fried, "Activity assessment of root caries lesions with thermal and near-infrared imaging methods," *J Biophotonics*, 10(3), 433-445 (2016).
- [22] V. B. Yang, D. A. Curtis, D. Fried, and "Use of Optical Clearing Agents for Imaging Root Surfaces with Optical Coherence Tomography " *IEEE J Sel Topics Quant Elect*, 25(1), 1-7 (2018).